Structural Elucidation of β-$(Y,Sc)_2Si_2O_7$: Combined use of ^{45}Sc and ^{89}Y MAS-NMR and powder diffraction

Allix M.,[1,2] Alba M.D.,[3] Florian P.,[1,2] Fernández A.J.,[3] Suchomel M.,[4] Escudero A.,[3] Suard E.[5] and Becerro A.I.[3*]

[1]CNRS, UPR3079 CEMHTI, 1D avenue de la Recherche Scientifique, 45071 Orléans cedex2, France.

[2]Université d'Orléans, Avenue du Parc Floral, BP 6749, 45067 Orléans cedex 2, France.

[3]Instituto de Ciencia de Materiales de Sevilla (CSIC-Universidad de Sevilla). c/ Américo Vespucio, 49. 41092 Sevilla (Spain).

[4]Argonne National Laboratory, Advanced Photon Source, Argonne, IL 60439 USA.

[5]Institut Max Von Laue Paul Langevin, F-38042 Grenoble 9, France.

Abstract

Although the structures of pure $Sc_2Si_2O_7$ and β-$Y_2Si_2O_7$ have been described in the literature using the *C2/m* space group, ^{29}Si MAS NMR measurements of the intermediate members of the $Sc_2Si_2O_7$ - β-$Y_2Si_2O_7$ system indicate a lowering of the symmetry to the *C2* space group. Indeed, these compositions exhibit a unique Si crystallographic site and a SiOSi angle lower than 180° non compatible with the *C2/m* space group. *C2* is the only alternative possible space group as *Cm* can be discarded regarding to its two different Si sites per unit cell. Moreover, ^{89}Y and ^{45}Sc MAS NMR data have revealed the existence of two different *RE* (*RE*= Sc, Y) sites in the structure of the intermediate members of the $Sc_2Si_2O_7$ - β-$Y_2Si_2O_7$ system, confirming the lowering of the symmetry to the *C2* space group. The viability of the *C2* model has then been tested and confirmed by refinement of synchrotron and neutron powder diffraction data for the different members of the system. The structural evolutions across the $Sc_2Si_2O_7$ - β-$Y_2Si_2O_7$ system are discussed.

Keywords

$Y_2Si_2O_7$, $Sc_2Si_2O_7$, rare earth silicates, ^{45}Sc and ^{89}Y MAS NMR spectroscopy, synchrotron, neutrons diffraction.

* Corresponding author: anieto@icmse.csic.es Tel no: +34 954489545; Fax no: +34 954460665

1.- Introduction

Rare Earth disilicates ($RE_2Si_2O_7$) exhibit different polymorphic forms depending on the *RE* ionic radius, temperature and pressure (Ito and Johnson, 1968; Felsche, 1973). $Y_2Si_2O_7$ shows, in particular, up to five polymorphs versus temperature at room pressure (y, α, β, γ and δ, also called respectively y, B, C, D and E,) while $Sc_2Si_2O_7$, or thortveitite, exhibits a unique polymorph (β also called C) up to the melting point of the compound.

A remarkable feature of the thortveitite structure is the unusual SiOSi angle, reported as 180º (Cruickshank et al. 1962; Smolin et al. 1973; Bianchi et al. 1988). There has been a considerable amount of discussion about the correctness of this structural model as the value of 180º is rather unusual for sorosilicates. Such angles are usually much smaller (130-140º; Liebau, 1986). The preference for a nonlinear structure with regard to the Si-O-Si bridge is supported by quantummechanical calculations (Meagher et al., 1979; Gibbs et al. 1981): the energy of a bent Si-O-Si link is shown to be smaller than for the linear *(180°)* counterpart. This discussion was also dealing with the question of whether the correct space group for thortveitite is *C2/m* or *C2*, both of them are possible on the basis of the diffraction symmetry. However, it was concluded that the correct space group for $Sc_2Si_2O_7$ is the centrosymmetric *C2/m*, as it provides the most consistent bond lengths and angles, in spite of a SiOSi angle of 180º (Cruickshank et al. 1962; Smolin et al. 1973; Bianchi et al. 1988).

The structure of β-$Y_2Si_2O_7$ was studied by Redhammer and Roth (2003), who initially refined it using the *C2* space group with acceptable residual values. However, the thermal parameters values for two of the four O atoms were definitely non-positive. Validation tests of the final *C2* structural model clearly showed the presence of additional symmetry (mirror plane), suggesting that *C2/m* was the correct space group. Thus, a new structural resolution was undertaken, revealing the known thortveitite structure type of β-$Y_2Si_2O_7$ and yielding better final residual values (with fewer refined parameters) and positive definite displacement parameters for all atoms.

The $Sc_2Si_2O_7$-β-$Y_2Si_2O_7$ system has been studied previously as a function of temperature and composition (Escudero et al. 2007). The particular behaviour of this system annealed at 1300ºC was analysed, showing a complete solid solubility of one member into the

other, with the β-$(Sc,Y)_2Si_2O_7$ structure type. Structural refinements for every member of the system were performed using the *C2/m* space group, as established in the literature for the end-members. All unit cell parameters were linear with composition, but the evolution of the c and β unit cell parameters did show a slope change at x~1.0. Likewise, SiOSi angles were obtained for the intermediate compositions of the system from ^{29}Si MAS NMR data (Escudero et al. 2007). These angles varied with composition, showing a minimum of 170.8º at x~ 1.0. This result implied that *C2/m* is not the space group of the intermediate members, as it forces the SiOSi angle to be equal to 180º.

Alternative possible space groups for the intermediate members are *C2* and *Cm*. Both of them allow SiOSi angles to differ from 180º, as suggested by the ^{29}Si MAS NMR data. However, *Cm* generates two different Si crystallographic sites, in opposition with the single Si site observed on the ^{29}Si MAS NMR spectra of the intermediate members (Escudero et al. 2007). On the other hand, the differences between the *C2/m* and *C2* structural models are very small. Both of them generate a unique Si crystallographic site. However, the *C2/m* model has a unique *RE* (*RE*= Sc, Y) site while in *C2*, two different *RE* sites exist, permitting a higher degree of distortion in the *C2* structure for the SiO_4 tetrahedron. In addition, there is a supplementary oxygen site in the *C2* model.

The aim of the present study is to analyse the structures across the $Sc_2Si_2O_7$ – β-$Y_2Si_2O_7$ system using complementary techniques that allow studying the structure at long and short range ordering. ^{45}Sc and ^{89}Y MAS NMR spectroscopy has been used to analyse the local environments of both nuclei. The MAS-NMR spectra inform on the number of *RE* crystallographic sites of the structures. In a second stage, and based on the NMR results, synchrotron and neutron powder diffraction refinement have been used to propose a structural model for the intermediate members of the system.

2.- Experimental

2.a.- Synthesis: The sol-gel route used for this study was derived from the synthesis of a well-homogenized gel of $Y_2Si_2O_7$ (Díaz et al. 2001). The starting materials were $Y(NO_3)_3{\cdot}6H_2O$ (99.9% Sigma), $Sc(NO_3)_3{\cdot}3H_2O$ (99.999% Sigma), $Si(OC_2H_5)_4$ (TEOS, 98% solution Sigma) and 96% ethanol. A TEOS solution in ethanol (1:3 in volume) was added over appropriate amounts of $Y(NO_3)_3{\cdot}6\ H_2O$ and $Sc(NO_3)_3{\cdot}3H_2O$ previously

dissolved in 5 mL ethanol for the preparation of $Sc_{2-x}Y_xSi_2O_7$ members with x = 0, 0.50, 1.00, 1.50, and 2.00. The mixtures were stirred at 40ºC until transparent gels were obtained. The gels were dried at 60ºC for 24 hours in air. Nitrates were eliminated by calcination at 500ºC for 1 hour at a heating rate of $1ºC \cdot min^{-1}$. The white powder obtained was subsequently calcined at a heating rate of $5°C \cdot min^{-1}$ up to 1300ºC for 24 hours and slowly cooled down to room temperature. These conditions allowed isolating the β-$(Sc,Y)_2Si_2O_7$ polymorph for all the solid solution compositions (Escudero et al. 2007). $(Y,Sc)_2SiO_5$ and SiO_2 were obtained in some compositions as subproducts.

2.b.- Characterization:

Magic Angle Spinning Nuclear Magnetic Spectroscopy: Magic Angle Spinning Nuclear Magnetic Spectroscopy: ^{45}Sc MAS experiments were carried on a Bruker Avance WB 750 MHz (17.6 T) spectrometer operating at 182.22 MHz. Powder samples were packed into 2.5mm zirconia rotors and spun at 30 kHz in a double resonance Bruker probe. The ^{45}Sc chemical shifts were referenced relative to a 1 M Scandium chloride solution with 3% HCl added. MAS experiments were obtained at a radio-frequency field ν_{rf} of 25 kHz using 0.5 µs pulse width (i.e. smaller than $\pi/24$ for quantitativity (Samoson et al. 1981)). The spin-lattice relaxation time T_1 was estimated to be 7 s with a saturation-recovery experiment and the recycle delays were set accordingly (Ernst et al. 1987). A spectral width of 2.5 MHz was used to avoid folding the spinning sidebands back into the spectrum, baseline correction being applied manually afterwards to remove the baseline oscillation induced by the 4.5 µs dead-time.

The ^{45}Sc 3Q MQMAS (Frydman et al. 1995, Medek et al. 1995) NMR experiments were performed spinning at 30.03 kHz in a 2.5 mm rotor and using a shifted-echo pulse sequence (Massiot et al. 1996). Excitation and mixing were done at ν_{rf} =150 kHz with pulse lengths of 1.2 µs and 0.4 µs respectively, the selective π pulse being applied at ν_{rf} = 7.5 kHz, the echo shift was 45 rotor periods (i.e. 1.5 ms and full-echo acquisition) and the recycle delay 5 s. In order to avoid sidebands in the indirect dimension the t_1 time increment was set to the rotor period 33.3 µs (Massiot 1996) and typically 30 t_1 increments were needed.

The ^{89}Y MAS experiments were performed on a Bruker Avance WB 300 MHz (7.0 T) operating at 14.7 MHz. Powdered samples were packed into 7mm silicon nitride rotors and spun at 4 kHz in a double resonance "low-γ" Bruker probe specifically design to work at low frequency. The ^{89}Y chemical shifts were referenced relative to a 1 M yttrium chloride solution. The spin-lattice relaxation time T_1 of $Y_2Si_2O_7$ was estimated to be 1300 s with a saturation-recovery experiment and hence for this compound a Hahn-echo experiment was used for a π/2 pulse of 39 µs, a recycle delay of 1650 s (Ernst et al. 1987) and 96 scans accumulated. We took advantage of the line broadening observed for $Sc_{2-x}Y_xSi_2O_7$ x = 1.5, 1.0, 0.5 and used a rotor-synchronized CPMG (Carr et al. 1954, Cheng et al. 1989, Cowans et al. 1993, Hung et al. 2004) sequence where trains of whole spin echoes are recorded to obtain an increase in signal-to-noise ratio with respect to a regular Hahn-echo sequence. We used π/2 pulses of 39 µs, acquiring between 30 and 60 echoes separated by 28 rotor periods (7.0 ms) with a recycle delay of 700 s and summing between 100 and 400 transients. The echo trains were not directly Fourier-transformed but rather the echoes were separated, convoluted with an adequate Gaussian line broadening, Fourier-transformed and summed to obtain the final spectra.

Diffraction techniques: High-intensity and high-resolution *synchrotron powder XRD* data have been recorded on the 11-BM diffractometer at the Advanced Photon Source (APS), Argonne National Laboratory. Data were collected over the 0.5-55° 2θ range with a 0.001°step size at room temperature using a wavelength of λ=0.413581Å. The sample was contained in a 0.5 mm capillary and was spun at 600 Hz during data collection.

Neutron powder diffraction patterns were recorded on the D2B high-resolution/high-flux powder diffractometer at the Institut Laüe-Langevin in Grenoble, France. The sample was packed in a vanadium can. Data were acquired with a λ=1.594Å wavelength at 2θ intervals of 0.05° over the $10^o < 2\theta < 160°$ angular range.

Diffraction patterns were analysed with the Rietveld method using the GSAS software (Larson and Von Dreele, 1994)**.** Refined parameters were: background coefficients, unit cell and profile parameters, atomic coordinates, site occupation factors, isotropic temperature factors and phase fractions. Anisotropic temperature factors were used for the refinement of the neutron data. Structural refinements have been performed using both

C2 and *C2/m* space groups. In the *C2* case, starting parameters were those given by Smolin et al. (1971) for β-$Yb_2Si_2O_7$. The Y/Sc ratios have been refined on the two sites, using constraints on the composition: Occ(Y1+Y2) (and Occ(Sc1+Sc2)) have been constrained to their nominal values in each sample. In the *C2/m* case, the starting parameters for the refinements of the $Y_xSc_{2-x}Si_2O_7$ structures with $x \leq 1$ were taken from those reported for pure β-$Sc_2Si_2O_7$ (Smolin et al. 1972) while the refinement of the $Y_xSc_{2-x}Si_2O_7$ structure with x = 1.5 was carried out from the parameters reported for pure β-$Y_2Si_2O_7$ (Redhammer and Roth, 2003). $(Y,Sc)_2SiO_5$ and SiO_2 have been added as secondary phases (no SiO_2 has been detected for the $YScSi_2O_7$ composition).

3.- Results

3.1.- Nuclear Magnetic Resonance results

3.1.1.- ^{89}Y MAS NMR results

Figure 1 (left) shows the experimental ^{89}Y MAS NMR spectra of β-$Y_xSc_{2-x}Si_2O_7$ samples with x = 0.5, 1.0, 1.5 and 2.0, which have been registered using CPMG technique to get a high S/N ratio. The spectrum of the Y-rich end-member, β-$Y_2Si_2O_7$ (Figure 1a), displays a narrow peak at 207.2 ppm with FWHM = 2.3 Hz, in good agreement with the literature (Becerro et al., 2004). The presence of a unique narrow ^{89}Y signal of β-$Y_2Si_2O_7$ indicates the existence of a unique Y crystallographic site in the structure, compatible with space group *C2/m* and a SiOSi angle of 180º, in agreement with previous structural studies on this compound (Redhammer and Ross, 2003). The spectra of the rest of compositions (Figures 1b-d) exhibit broad and asymmetric bands that point to the presence of more than one Y resonance. This result implies the existence of more than one Y crystallographic site in the unit cell of the intermediate members and points to a *C2* space group, which contains two different RE crystallographic sites in the unit cell. The maximum of the band shifts towards higher frequency as the Y content decreases. The spectrum of β-$Y_{0.5}Sc_{1.5}Si_2O_7$ shows, in addition, two low intensity signals at 155.6 and 240.7 ppm corresponding to Y in the *X2*-$(Sc,Y)_2SiO_5$ phase, which is a subproduct of the synthesis, as commented in the Experimental section. These signals are also present in the rest of the intermediate compositions spectra, but are not clearly observed because of the high FWHM of the resonances.

The ^{89}Y MAS CPMG spectra have been simulated (Figure 1, right) with the resonances corresponding to the expected Y sites in the structure (two sites for the intermediate compositions and a unique site for the end-member). The results are displayed in Table 1. The simulation included two additional resonances accounting for two Y sites in *X2*-$(Sc,Y)_2SiO_5$ (Becerro et al. 2004). The ^{89}Y chemical shift of one of the Y sites of β-$(Y,Sc)_2Si_2O_7$ does vary linearly with composition (open circles in Figure 2), and the chemical shift of the single Y site in pure β-$Y_2Si_2O_7$ is located in the extrapolation of that line. The second Y site does not show a linear dependence with composition (solid circles in Figure 2). On the other hand, the area under the curve of each resonance indicate that $Sc_{2-x}Y_xSi_2O_7$ members with x=1.0 and x= 1.5 show a homogeneous distribution of Y between both sites, while the x= 0.5 composition shows a preferential occupation of Y for one of the crystallographic sites, in good agreement with diffraction results, as will be shown below.

3.1.2.- ^{45}Sc MAS NMR results

Figure 3a and 3b show the two-dimensional ^{45}Sc (3Q) MAS NMR spectra of samples $Y_xSc_{2-x}Si_2O_7$ with x = 0.0 and x = 1.0, respectively. The number of the different Sc sites has been extracted from the isotropic dimension of these ^{45}Sc MQMAS spectra. The isotropic dimension of the MQMAS spectrum of pure β-$Sc_2Si_2O_7$ (Figure 3c) shows a single contribution compatible with a unique Sc site in the unit cell and a *C2/m* space group, in agreement with the structural studies of this compound (Cruickshank et al. 1962; Smolin et al. 1973; Bianchi et al. 1988). However, two Gaussian lines were necessary to fit the isotropic spectrum of the β-$ScYSi_2O_7$ composition (Figure 3d), which are likely due to two different Sc sites. This result implies a lowering of the symmetry for this intermediate composition which allows the existence of two Sc sites, in agreement with the ^{89}Y NMR results. The unique possibility conserving the unit cell metric is the *C2* space group.

Figure 4 shows the single pulse ^{45}Sc MAS NMR spectra of the $Y_xSc_{2-x}Si_2O_7$ samples. Adding Y to $Sc_2Si_2O_7$ progressively smoothen the characteristic discontinuities of the Sc NMR lineshapes, indicating a progressive increase of disorder. The SP ^{45}Sc MAS NMR spectra have been simulated with the resonances corresponding to the expected Sc sites

in the structure (two sites for the intermediate compositions and a unique site for the end-member), and the results (isotropic chemical shifts, quadrupolar coupling constants, asymmetry parameter and area under the curve of each resonance) are displayed in Table 2. The areas under the curve show a homogeneous distribution of Sc in both sites for $x \geq 1.0$, in agreement with the ^{89}Y MAS NMR data, and the diffraction data, as shown below. On the other hand, Figures 5a and 5b show the ^{45}Sc weighted mean isotropic chemical shift and quadrupolar coupling constants values, respectively, versus composition, obtained from the simulation of the MQMAS spectra. Both parameters decrease linearly with increasing Y content, as expected in the case of a solid solution of β-$Y_2Si_2O_7$ in $Sc_2Si_2O_7$.

3.2.- Diffraction results

Based on the ^{89}Y and ^{45}Sc NMR data described above which suggest the existence of two different *RE* crystallographic sites, as well as on the ^{29}Si MAS NMR data published in Escudero et al. (2007), which indicate the existence of a unique Si crystallographic site coupled to a non linear SiOSi angle, C2 appears to be the only alternative possible space group. In fact, *Cm*, giving the same reflection conditions, can be discarded regarding to its two different Si sites per unit cell. The viability of the *C2* space group, compatible with these NMR data, will now be demonstrated by refinement of the structure under this space group from synchrotron and neutron powder diffraction patterns. Refinements using C2/m have also been included for a comparison purpose.

3.2.1.- Study of the intermediate members of the system

3.2.1.1.- Synchrotron powder diffraction

Structural refinements have been performed for $Y_xSc_{2-x}Si_2O_7$ compositions with x = 0.5, 1.0 and 1.5, using both *C2* and *C2/m* space groups models. Figure 6 shows the experimental and fitted patterns for $Y_{0.5}Sc_{1.5}Si_2O_7$, using space groups *C2* (fig. 1a) and *C2/m* (fig. 1b). The fittings of the two other compositions are very similar and are not shown. Tables 3, 4 and 5 show the atomic parameters obtained for the three compositions using space groups *C2* and *C2/m*. Refinements using *C2* space group indicate a preferential occupation of Y and Sc for one of the *RE* sites in the $Sc_{2-x}Y_xSi_2O_7$ with x= 0.5 composition, while the two other samples show a homogeneous distribution of Sc and Y between both crystallographic sites, in good agreement with the NMR data (asterisks

in Tables 3, 4 and 5 indicate the site occupation factors expected in case of homogeneous distribution of Sc and Y between both *RE* sites).

Figures 7a and 7b are views of the structures obtained for $YScSi_2O_7$ using space groups *C2* and *C2/m*. SiOSi angles obtained from the refinements in *C2* were respectively 164.4(3)º, 167.2(3)º and 166.4(2)º for $Y_{0.5}Sc_{1.5}Si_2O_7$, $YScSi_2O_7$ and $Y_{1.5}Sc_{0.5}Si_2O_7$ compositions. The three values are lower than 180º, as calculated from ^{29}Si NMR data (Escudero et al. 2007). Figure 7c is a Fourier map obtained by summing the Fobs from 0.35 to 0.65 along z of the $YScSi_2O_7$ pattern. The deviation of the SiOSi angle from 180º is clearly observed.

These results demonstrate that the refinements using the *C2* space group are possible and stable for the intermediate compositions. Reliability factors are quite good in both space groups (Table 6) although, in terms of fit quality, there is no real difference between the two space group refinements. Thus, synchrotron XRD data refinements indicate that the *C2* model is possible for the intermediate members of the β-$(Sc,Y)_2Si_2O_7$ system, as suggested by ^{89}Y and ^{45}Sc MAS NMR data.

3.2.1.2.- Neutron powder diffraction

Neutron diffraction data refinements performed on $YScSi_2O_7$ composition were also possible in both *C2* and *C2/m* space groups. Figure 8 shows the experimental and fitted patterns for $YScSi_2O_7$, using space groups *C2* (fig. 8a) and *C2/m* (fig. 8b). Reliability factors (Table 6) are quite good in both space groups but, again, in terms of fit quality, there is no real difference between the two space group refinements. Table 7 shows the atomic parameters obtained for this composition. The SiOSi angle obtained from the refinements in *C2* was 169.2(17)º, in good agreement with the synchrotron data.

3.2.2. Study of the end-members of the system

Although the set of ^{89}Y and ^{45}Sc MAS NMR and diffraction data on the intermediate members strongly suggest a *C2* model, an extra argument to ensure that the non 180º values of the SiOSi angles of the intermediate compositions are real and probably linked to the *C2* space group would be to obtain angle values close to 180º for the $Sc_2Si_2O_7$ and β-$Y_2Si_2O_7$ end members when refined in *C2*, even if it has been proved that this is not the

proper symmetry for these compositions (Bianchi et al. 1988; Redhammer and Roth, 2003).

Synchrotron powder diffraction patterns were recorded with this purpose on $Sc_2Si_2O_7$ and β-$Y_2Si_2O_7$ compositions and the structures were refined using the *C2* space group structural model. Refinements are possible in *C2* for both compositions. In the $Sc_2Si_2O_7$ case, a SiOSi angle value very close to 180º was obtained (179.5(1)º). Because when lowering the symmetry the SiOSi angle converges to the linear 180° value, this means that *(i)* the refinement is in good agreement with the *C2/m* choice for the scandium end members and *(ii)* refinements using the *C2* model are a good indication of the symmetry (*C2* or *C2/m* space group) via the SiOSi angle value.

However, this was not exactly the case for β-$Y_2Si_2O_7$, where the SiOSi angle refined value was 177.2(5)º. This result, though close to 180° and far from the values obtained for the intermediate compositions (164-167°), is not entirely conclusive. It could be linked to the fact that X-rays are not very sensitive to light elements like oxygen, especially when a heavy atom like Yttrium is present in the structure. In order to overcome this disadvantage and obtain more accuracy on the SiOSi angle value, we have recorded neutron powder diffraction pattern of the β-$Y_2Si_2O_7$ composition. Indeed neutron scattering lengths of the different species (Y, Si and O) are much closer than the X-ray ones for which Y is from far predominant. Structure solution for β-$Y_2Si_2O_7$ using the neutron diffraction data has thus been performed in *C2* space group, leading to a 179.1(16)º value for the SiOSi angle and so confirming our previous results .

4.- Conclusions

^{89}Y and ^{45}Sc MAS NMR spectroscopy indicate the existence of a unique *RE* (Sc, Y) crystallographic site in the unit cell of the end members of the $Sc_2Si_2O_7$-β-$Y_2Si_2O_7$ system, while the spectra of the intermediate members point to the presence of two different *RE* sites. Morevover, ^{29}Si MAS NMR measurements of the intermediate members show a unique Si crystallographic site and a SiOSi angle lower than 180° non compatible with the *C2/m* space group. These results suggest that although *C2/m* is the space group of the end members, the intermediate members crystallizing in a lower symmetry space group. The viability of the *C2*, the only alternative space group matching

the NMR results requirements has been demonstrated by means of synchrotron and neutron powder diffraction data.

Acknowledgments

ILL beamtime was obtained using the EASY access system (http://www.ill.eu/users/applying-for-beamtime/easy-easy-access- system/; proposals EASY57 and EASY58 on D2B). Use of the Advanced Photon Source at Argonne National Laboratory was supported by the US Department of Energy, Office of Science, Office of Basic Energy Sciences, under contract No. DE-AC02-06CH11357. AJF-C gratefully acknowledges an FPDI grant from Junta de Andalucía. This work is also supported by the European Union VI Framework Programme as an HRM Activity (contract No. MRTN-CT-2006-035957), DGICYT (project No. CTQ2010-14874/BQU) and Junta de Andalucı´a JA FQM 06090.

References

Becerro AI, Escudero A., Florian P., Massiot D. and Alba M.D. Revisiting $Y_2Si_2O_7$ and Y_2SiO_5 polymorphic structures by ^{89}Y MAS-NMR spectroscopy. J. Solid State Chemistry 177, 2783-2789 (2004)

Bianchi R., Pilati T., Diella V., Gramaccioli C.M. and Mannucci G. Am. Mineral. 73 (1988) 601-607

Carr H. Y., Purcell E. M., Phys Rev 94 (1954) 630-638

Cheng J. T., Ellis P. D., J. Phys. Chem. 93 (1989) 2549-2555

Cowvans B. A., Grutzner J. B., J. Magn. Reson. A 105 (1993) 10-18

Cruickshank D.W.J., Lynton H. and Barclay G.A., Acta Cryst. 15 (1962) 491-498

Díaz M., García-Cano I., Mello-Castanho S., Moya J.S., Rodríguez M.A., J. Non-Cryst. Solids 289 (2001) 151

Ernst R., Bodenhausen G., Wokaun A., Principles of Nuclear Magnetic Resonance in One and Two Dimensions; Oxford University Press, New York, 1987.

Escudero A., Alba M.D. and Becerro A.I., J. Solid State Chem. 180 (2007) 1436-1445

Felsche J. Str. Bond. 13 (1973) 99

Frydman L., Hardwood J. S., J. Am. Chem. Soc. 117 (1995) 5367

Gibbs, G.V., Meagher, E.P., Newton, M.D., and Swanson, D.K. (1981) A comparison of experimental and theoretical bond length and angle variations for minerals, inorganic solids, and molecules in structure and bonding of crystals, vol. I, p. 195-225. Academic Press, New York.

Hung I. Rossini A. J., Schurko R. W., J. Phys. Chem. A 108 (2004) 7112-7120

Ito J. and Johnson H. Am. Mineral. 53 (1968) 1940

Larson A.C. and Von Dreele R.B. *GSAS: General Structural Analysis system*, Los Alamos National Laboratory, Los Alamos, NM. The Regents of the University of California, 1994

Liebau F. Structural Chemistry of Silicates, Berlin: Springer Verlag, 1986

Massiot D., Touzo B., Trumeau D., Coutures J.-P., Virlet J., Florian P., Grandinetti P.J., Solid. State Nuc. Magn. Reson. 6(1) (1996) 73-83

Massiot D., J. Magn. Reson. A 122 (1996) 240-244

Meagher, E.P., Tossell, J.A., and Gibbs, G.V. Phys. Chem. Miner., 1979, 4, 11-21.

Medek A., Harwood J. S., Frydman L. J., Am. Chem. Soc. 117 (1995) 12779.

Meiboom S., Gill D., Rev. Sci. Instrum. 29 (1958) 688-691

Redhammer G.J. and Roth G. Acta Cryst. C59 (2003) 103-106

Samoson A., Lippmaa E., Phys. Rev. B 28 (1983) 6567

Smolin Y.I., Shepelev Y.F., Butikova I.K, Zh. Strukt. Khim. 12 (1971) 272

Smolin Y.I., Shepelev Y.F., Titov A.P. Kristallografiya 17 (1972) 857

Smolin Yu. I., Shepelev Yu.F. and Titiov A.P. Sov. Phys. Crystallogr. 17 (1973) 749-750

Figures

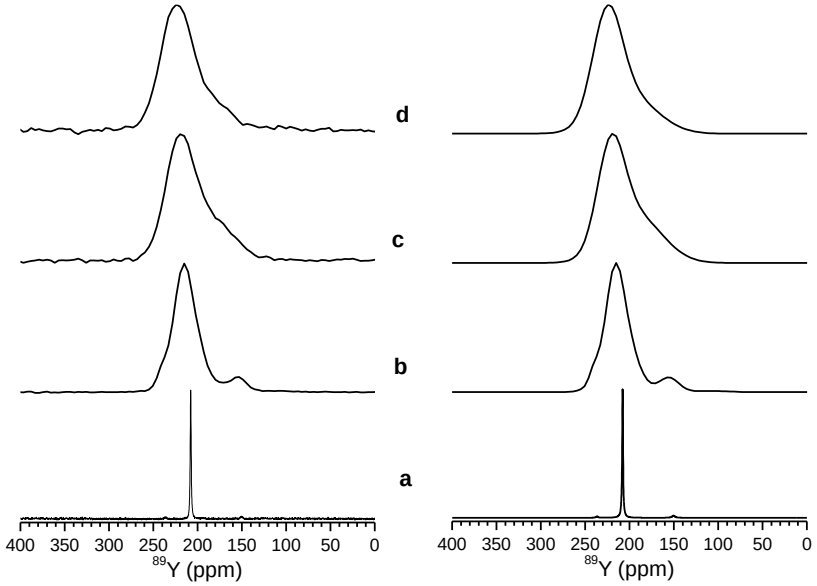

Figure 1. Experimental (left) and fitted (right) ^{89}Y CPMG NMR spectra of $Y_xSc_{2-x}Si_2O_7$ with x = 2.0 (a), 1.5 (b), 1.0 (c) and 0.5 (d).

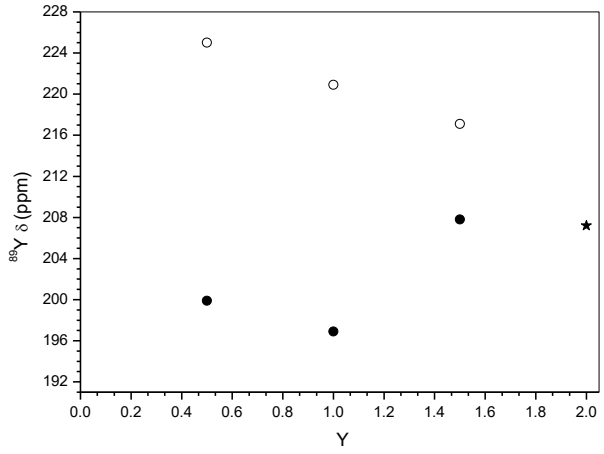

Figure 2. ^{89}Y chemical shifts of the individual contributions of Fig. 1 right *vs.* nominal composition. Open and solid circles represent the two different Y sites in the intermediate members. The star corresponds to the chemical shift of the unique Y site in the Y-rich end-member.

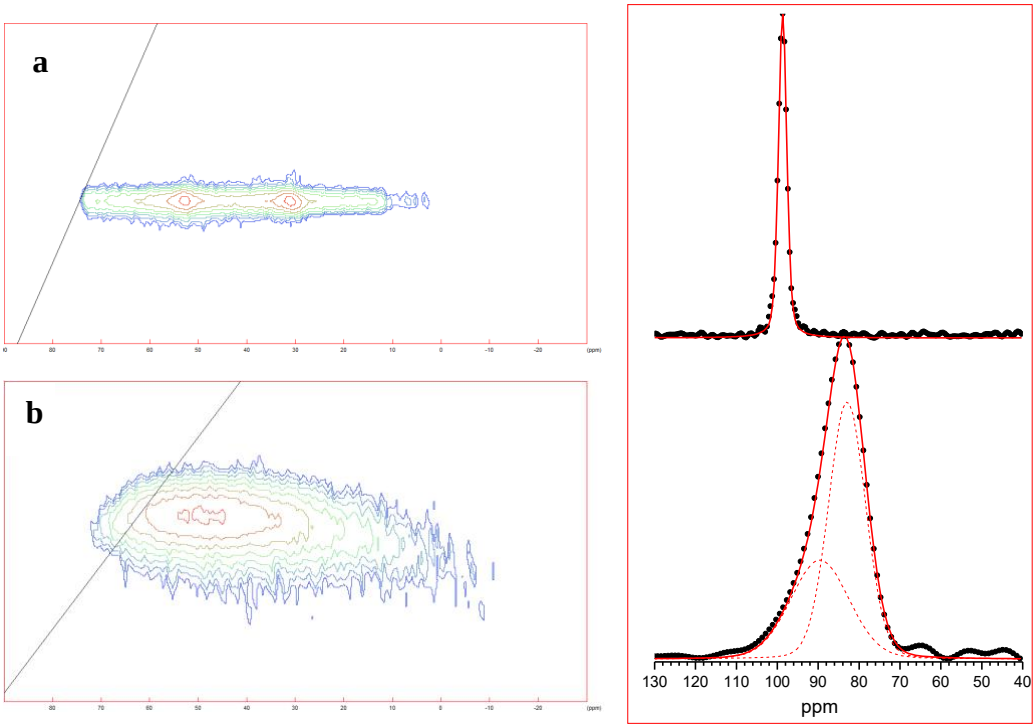

Figure 3. Two-dimensional ^{45}Sc (3Q) MAS NMR spectra of samples $Y_xSc_{2-x}Si_2O_7$ with x = 0.0 (a), 1.0 (b). c and d) Isotropic projection of the 2D signal of spectra a and b, respectively.

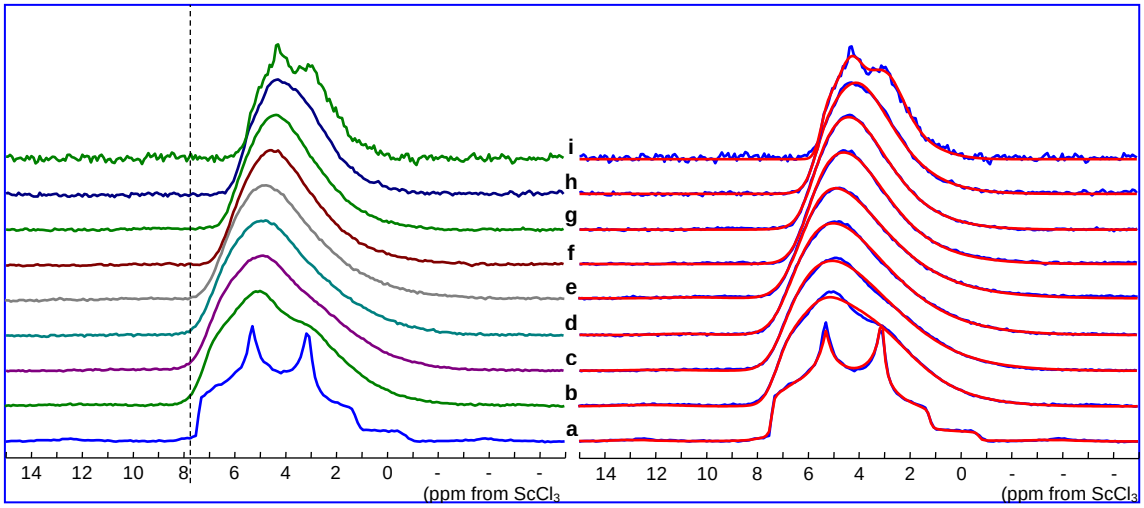

Figure 4. Raw and fitted ^{45}Sc (SP) MAS NMR spectra of samples $Y_xSc_{2-x}Si_2O_7$ with x = 0.0 (a), 0.2 (b), 0.4 (c), 0.6 (d), 1.0 (e), 1.3 (f), 1.5 (g), 1.7 (h) and 1.9 (i).

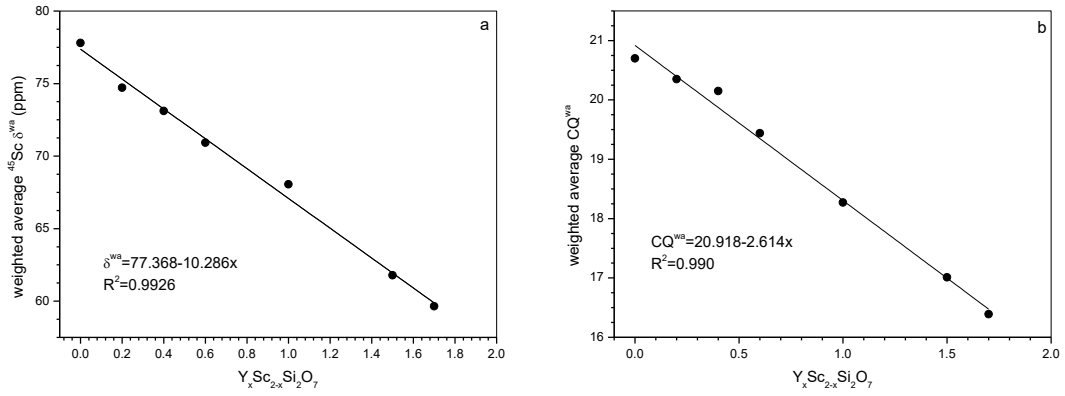

Figure 5. a) ^{45}Sc weighted average isotropic chemical shift vs. nominal composition, and, b) ^{45}Sc weighted average CQ values evolution vs. nominal composition, obtained from ^{45}Sc MQMAS spectra.

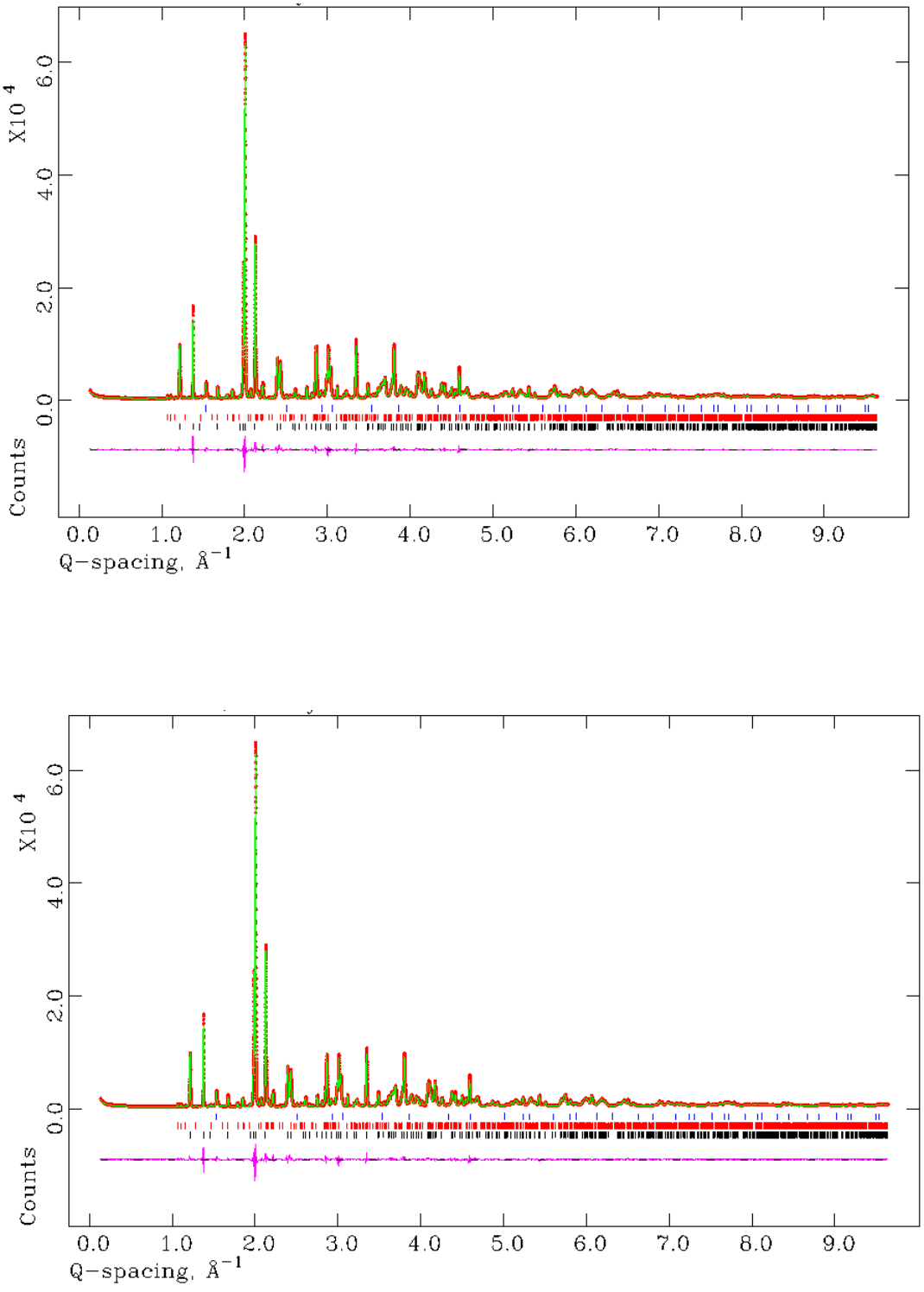

Figure 6: Experimental (dots) and fitted (solid line) synchrotron patterns recorded on the 11BM station (APS, USA), for $Y_{0.5}Sc_{1.5}Si_2O_7$, using a) space group *C2* and b) space group *C2/m*. The difference curves are also included.

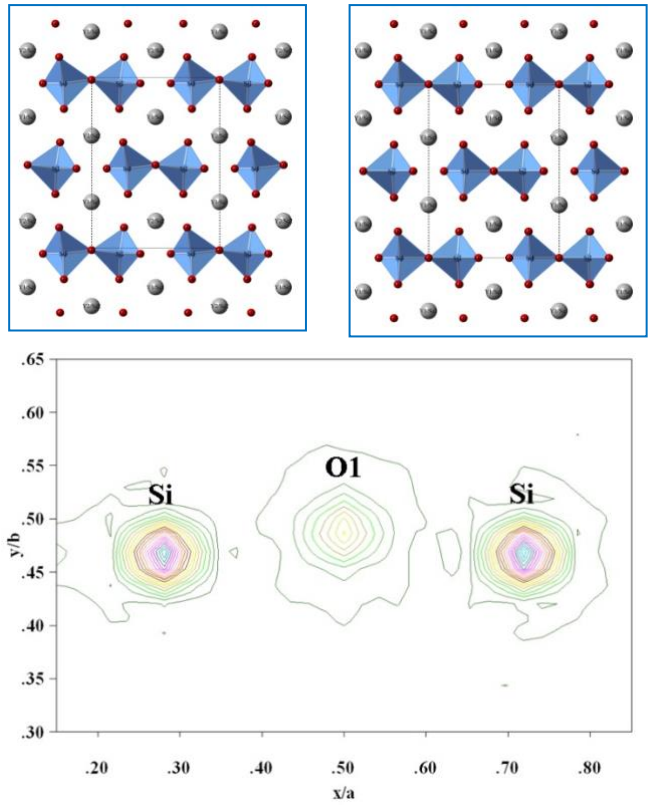

Figure 7: a) and b): views of the structures of $YScSi_2O_7$ using, respectively, space groups *C2* and *C2/m*. Data obtained from structure refinement of synchrotron data. c) Fourier map of $YScSi_2O_7$ along z; deviation of the SiOSi angle from 180º is clearly observed.

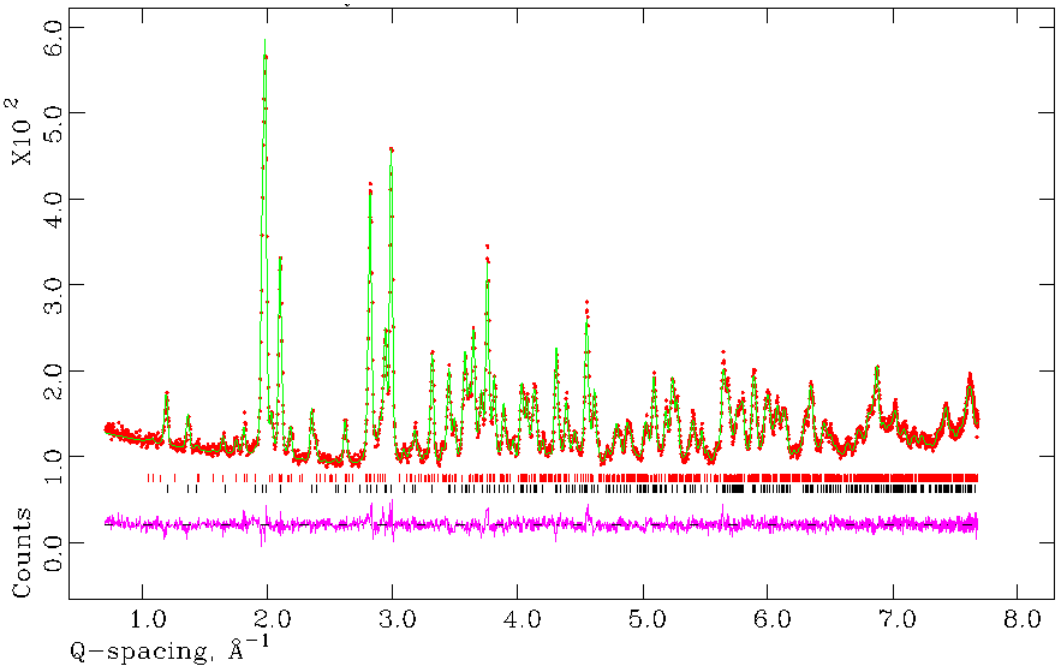
X10 2
6.0
5.0
4.0
3.0
2.0
1.0
0.0
Counts
1.0
2.0
3.0
4.0
5.0
6.0
7.0
8.0
Q−spacing, Å−1

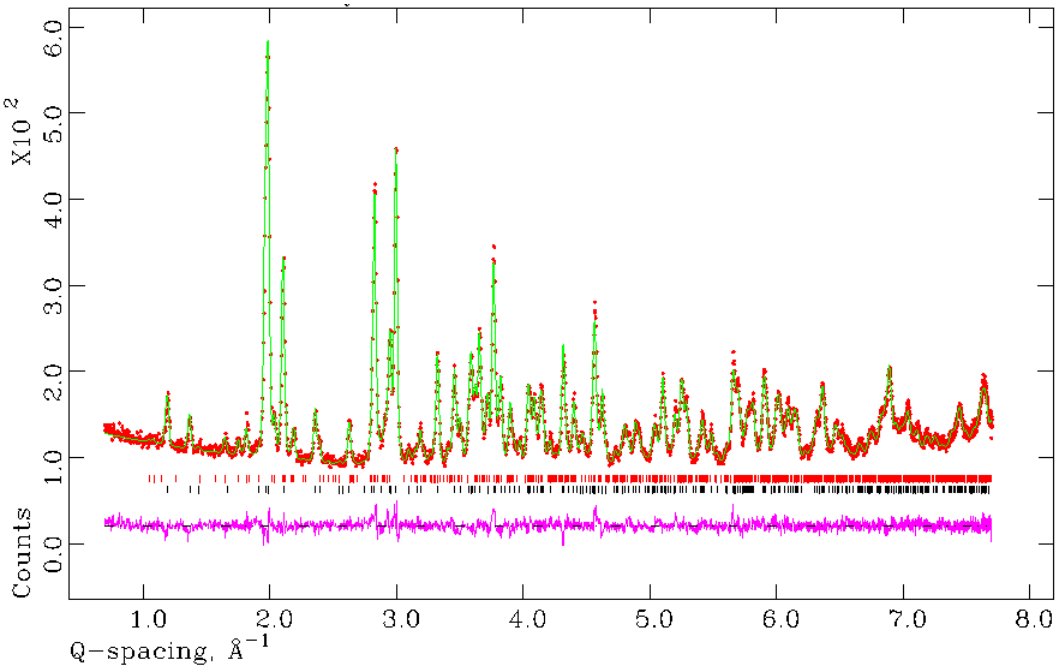
X10 2
6.0
5.0
4.0
3.0
2.0
1.0
0.0
Counts
1.0
2.0
3.0
4.0
5.0
6.0
7.0
8.0
Q−spacing, Å−1

Figure 8: Experimental (dots) and fitted (solid line) neutron patterns recorded at the D2B station (ILL, Grenoble, France), for $YScSi_2O_7$, using a) space group *C2* and b) space group *C2/m*. The difference curves are also included.

Table 1. ^{89}Y MAS NMR fit parameters for β-$Y_xSc_{2-x}Si_2O_7$

x (β-$Y_xSc_{2-x}Si_2O_7$)	δ (ppm)	$\Delta_{1/2}$ (ppm)	Area under the curve (%)
0.5	199.9	64.0	34.6
	225.0	38.5	65.4
1.0	196.9	65.9	50.2
	220.9	34.7	49.8
1.5	207.8	35.3	51.6
	217.1	23.5	48.4
100	207.2	2.3	100

Table 2. ^{45}Sc SP MAS NMR fit parameters for β- $Y_xSc_{2-x}Si_2O_7$

x β-$Y_xSc_{2-x}Si_2O_7$	δ_{iso} (ppm)	C_Q (MHz)	η	Area under the curve (%)
0.0	77.8	20.70	0.45	100
0.2	81.2	16.00	0.01	7.9
	75.3	20.95	0.43	92.1
0.4	77.1	16.47	0.23	16.9
	72.3	20.90	0.44	83.1
0.6	74.1	16.32	0.34	20.7
	70.1	20.26	0.47	79.3
1.0	69.6	16.22	0.60	56.9
	66.0	20.97	0.60	43.1
1.5	63.8	14.94	0.60	42.4
	60.3	18.54	0.60	57.6
1.7	62.5	14.08	0.60	19.2
	58.9	16.92	0.60	80.9

Table 3a. Refined atomic coordinates for $Y_{0.5}Sc_{1.5}Si_2O_7$ from synchrotron powder diffraction (11BM-APS) data collected at RT (space group *C2*; a=6.62050(6)Å; b=8.61152(7)Å; c=4.67462(3)Å and β=102.366(1)°). Asterisk indicates site occupation factors expected in case of homogeneous distribution of Sc and Y between both RE sites.

Atom	Site	x	y	Z	U_{iso} (*100)	Occ.
Y1/Sc1	2b	0.5	0.8055	0	0.44(6)	0.335(4)/0.665(4) (0.25/0.75)*
Y2/Sc2	2b	0.5	0.1935(1)	0	0.66(7)	0.165(4)/0.835(4) (0.25/0.75)*
Si	4c	0.7205(1)	0.5034(4)	0.4109(1)	0.51(2)	1
O1	2a	0.5	0.4778(4)	0.5	1.23(2)	1
O2	4c	0.8854(2)	0.4992(7)	0.7188(2)	1.23(2)	1
O3	4c	0.7297(6)	0.6473(4)	0.2276(8)	1.23(2)	1
O4	4c	0.7428(6)	0.3392(4)	0.2183(8)	1.23(2)	1

Table 3b. Refined atomic coordinates for $Y_{0.5}Sc_{1.5}Si_2O_7$ from synchrotron powder diffraction (11BM-APS) data collected at RT (space group *C2/m*; a=6.62047(6)Å; b=8.61153(7)Å; c=4.67465(3)Å and β=102.366(1)°).

Atom	Site	x	y	Z	U_{iso} (*100)	Occ.
Y/Sc	4g	0	0.30614(4)	0	0.52(1)	0.25/0.75
Si	4i	0.2212(1)	0	0.4107(1)	0.52(2)	1
O1	2c	0	0	0.5	1.48(2)	1
O2	4i	0.3847(2)	0	0.7192(2)	1.48(2)	1
O3	8j	0.2367(1)	0.1539(1)	0.2233(1)	1.48(2)	1

Table 4a. Refined atomic coordinates for $YScSi_2O_7$ from synchrotron powder diffraction (11BM-APS) data collected at RT (space group *C2*; a=6.71363(3)Å; b=8.72253(5)Å; c=4.67973(3)Å and β=102.084(1)°). Asterisk indicates site occupation factors expected in case of homogeneous distribution of Sc and Y between both RE sites.

Atom	Site	x	y	Z	U_{iso} (*100)	Occ.
Y1/Sc1	2b	0.5	0.76960	0	0.66(6)	0.50(1)/0.50(1) (0.50/0.50)*
Y2/Sc2	2b	0.5	0.15906(5)	0	0.40(6)	0.50(1)/0.50(1) (0.50/0.50)*
Si	4c	0.72062(7)	0.4663(4)	0.4131(1)	0.64(1)	1
O1	2a	0.5	0.4871(3)	0.5	1.30(2)	1
O2	4c	0.8809(1)	0.4659(7)	0.7163(2)	1.30(2)	1
O3	4c	0.7534(3)	0.6204(3)	0.2227(6)	1.30(2)	1
O4	4c	0.7161(3)	0.3164(3)	0.2213(6)	1.30(2)	1

Table 4b. Refined atomic coordinates for $YScSi_2O_7$ from synchrotron powder diffraction (11BM-APS) data collected at RT (space group *C2/m*; a=6.71352(3)Å; b=8.72241(5)Å; c=4.67975(3)Å and β=102.084(1)°).

Atom	Site	x	y	Z	U_{iso} (*100)	Occ.
Y/Sc	4g	0	0.30527(2)	0	0.51(1)	0.5/0.5
Si	4i	0.22097(6)	0	0.41264(9)	0.71(1)	1
O1	2c	0	0	0.5	1.81(2)	1
O2	4i	0.3817(1)	0	0.7165(2)	1.81(2)	1
O3	8j	0.2345(1)	0.1523(1)	0.2225(1)	1.81(2)	1

Table 5a. Refined atomic coordinates for $Y_{1.5}Sc_{0.5}Si_2O_7$ from synchrotron powder diffraction (11BM-APS) data collected at RT (space group *C2*; a=6.80085(7)Å; b=8.85057(9)Å; c=4.70109(4)Å and β=101.854(1)°). Asterisk indicates site occupation factors expected in case of homogeneous distribution of Sc and Y between both RE sites.

Atom	Site	x	y	Z	U_{iso} (*100)	Occ.
Y1/Sc1	2b	0.5	0.8244	0	0.68(10)	0.71(1)/0.29(1) (0.75/0.25)*
Y2/Sc2	2b	0.5	0.2143(1)	0	0.37(9)	0.79(1)/0.21(1) (0.75/0.25)*
Si	4c	0.7204(1)	0.5223(10)	0.4144(2)	0.53(3)	1
O1	2a	0.5	0.5005(6)	0.5	1.21(4)	1
O2	4c	0.8726(2)	0.5185(21)	0.7094(3)	1.21(4)	1
O3	4c	0.7477(8)	0.6717(8)	0.2279(15)	1.21(4)	1
O4	4c	0.7222(8)	0.3714(8)	0.2204(15)	1.21(4)	1

Table 5b. Refined atomic coordinates for $Y_{1.5}Sc_{0.5}Si_2O_7$ from synchrotron powder diffraction (11BM-APS) data collected at RT (space group *C2/m*; a=6.80082(7)Å; b=8.85048(9)Å; c=4.70108(4)Å and β=101.854(1)°).

Atom	Site	x	y	Z	U_{iso} (*100)	Occ.
Y/Sc	4g	0	0.30519(4)	0	0.51(1)	0.75/0.25
Si	4i	0.2203(1)	0	0.4142(2)	0.54(2)	1
O1	2c	0	0	0.5	1.49(3)	1
O2	4i	0.3735(2)	0	0.7105(3)	1.49(3)	1
O3	8j	0.2358(2)	0.1504(1)	0.2252(2)	1.49(3)	1

Table 6. Reliability factors obtained from structural refinements of powder synchrotron and neutron diffraction patterns.

	Synchrotron diffraction (11BM)				Neutron diffraction (D2B)			
	R_{wp}	R_p	R_F^2	χ^2	R_{wp}	R_p	R_F^2	χ^2
$Sc_2Si_2O_7$								
C2	8.22%	6.42%	2.32%	7.57	Non recorded			
C2/m	8.27%	6.46%	2.53%	7.66				
$Y_{0.5}Sc_{1.5}Si_2O_7$								
C2	7.20%	5.32%	2.65%	6.49	Non recorded			
C2/m	7.34%	5.46%	2.85%	6.75				
$YScSi_2O_7$								
C2	4.25%	3.39%	1.43%	1.82	3.55%	2.84%	3.03%	1.75
C2/m	4.41%	3.55%	1.65%	1.97	3.59%	2.85%	3.09%	1.80
$Y_{1.5}Sc_{0.5}Si_2O_7$								
C2	7.23%	5.37%	1.63%	4.90	Non recorded			
C2/m	7.30%	5.46%	1.76%	4.99				
$Y_2Si_2O_7$								
C2	6.60%	5.16%	1.61%	4.01	3.64%	2.97%	2.43%	1.94
C2/m	6.65%	5.19%	1.64%	4.05	3.66%	2.99%	2.03%	1.95